I.A.U
Karaj branch

Journal of
A p p l ied
C hemical
R esearch
jacr.kiau.ac.ir

Journal of Applied Chemical Research, 17, 1, 37-59 (2023)

Preparation of Novel Thermo-sensitive Polymer/βCD/WS_2 Nano-carriers for *invitro* Drug Release of Tamoxifen in the Presence and Absence of Near-Infrared (NIR) Laser

Abbas Bohloli, Maryam Daghighi Asli*, Elham Moniri, Azar Bagheri

Department of Chemistry, Central Tehran Branch, Islamic Azad University Tehran, Iran

(Received 14 May 2022; Final revised received 18 Aug. 2022)

Abstract

In this work, two novel N-isopropylacrylamide (NIPAA)/Beta-cyclodextrin (β-CD)/WS_2 and NIPAA/N, N-dimethyl acrylamide (DMAA)/WS_2/βCD nanocarriers were prepared for in vitro tamoxifen drug release in the absence and presence of Near-Infrared (NIR) laser. The characterization of resulting nanocarriers was carried out using X-ray diffraction (XRD), Fourier transforms infrared spectroscopy (FTIR), field-emission scanning electron microscopy (FE-SEM), and thermogravimetric analysis (TGA). To study the effect of temperature on drug release for chemotherapy, tamoxifen drug release was comparatively evaluated at three different temperatures (25, 37, and 50°C) with pH 7.4 in the absence of a NIR laser. It was found that tamoxifen release from the synthesized nanocarriers at 50°C was significantly greater than that at 25 and 37°C. To investigate the effect of laser light on drug release for chemo-photothermal therapy, the in vitro release tests were carried out at 37°C with a NIR laser light and with a power density of 1 W/cm^2 for 5 min. The increase of tamoxifen release after a laser light was 29.8% and 48.4%for NIPAA/βCD/WS_2 and NIPAA/DMAA/βCD/WS_2 samples, respectively. Thus, the combination of chemo/photothermal therapy had a synergistic effect on the drug release of tamoxifen. Furthermore, the total drug release of NIPAA/DMAA/βCD/WS_2 was greater than that of NIPAA/βCD/WS_2 nanocarrier. Furthermore, the kinetic release data were analyzed using Zero-order, First-order, Ritger-Peppas, and Higuchi models which followed the zero-order kinetic release model. Also, good stability was observed for tamoxifen in the drug release system.

Keywords: Thermosensitive Polymer, WS_2 nanosheet, Tamoxifen Release, Near-Infrared laser, kinetic models.

*__Corresponding author__: *Maryam Daghighi Asli, Department of Chemistry, Central Tehran Branch, Islamic Azad University Tehran-Iran. Email: daghighi1350@gmail.com. Phone: +98-9127375033.*

Introduction

Chemotherapy denotes a major therapeutic method for cancer treatment [1, 2]. Tamoxifen is an effective drug during the chemotherapy of breast cancer treatment and as an inhibitor agent after surgery[3]. Indeed, estrogen binds to hormone receptors leading to cell proliferation in the breast tissue. Tamoxifen is a selective estrogen receptor modulator that attaches to hormone receptors in the cancer cells and blocks the estrogen and the cancer is stopped[4]. The tamoxifen drug can decrease the risk and recurrence of breast cancer in premenopausal and postmenopausal women. Furthermore, the prevention of bone loss after menopause and the reduction of cholesterol levels are the other benefits of taking tamoxifen[3, 4]. However, there are some undesirable side effects to normal cells due to the aimless and nonspecific delivery of cancer drugs and insufficient dose of a cancer drug to destroy cancerous cells [2].

To overcome the mentioned limitations and difficulties, some methods have been developed. One of these methods is targeted drug delivery [5] leading to the higher availability of drugs to cancer cells and the significant reduction of serious side effects [6, 7]. The use of cancer drugs such as tamoxifen in traditional methods has been limited because traditional methods typically suffer systemic toxicity leading to hair thinning, fatigue, cerebrovascular event, bone pain, etc. [8]. To reduce the side effects and enhance therapeutic efficacy, nanoscale drug carriers have been used in drug delivery systems because of superior selective accumulation in tumor tissues[9, 10]. Furthermore, the combination of chemotherapy with other treatment methods such as photothermal therapy is another effective method to minimize the severe side effects [2, 11]. There are several limitations of applying single photothermal therapy such as the limited depth of light penetration, inhomogeneous accumulation in the cancerous tissues, and insufficient heat delivery in targeted tissues leading to incomplete tumor ablation [12-15]. Therefore, a synergistic chemo-photothermal therapy with an effective NIR absorbing agent, drug, and nanocarrier can be handled [12].

Recently, layered transition metal dichalcogenides nanosheets such as TaS_2, MoS_2, ReS_2, and WS_2 have been applied as NIR absorbing agents in drug delivery systems because of the high surface area, small band gap, and high NIR absorbance for effective hyperthermia generation under laser light [13, 16, 17]. Furthermore, these metal sulfide nanomaterials possess a good ability to load hydrophobic aromatic drugs such as tamoxifen on their surface [3, 13]. Nevertheless, the biomedical application of these nanosheets can be limited owing to the inherent hydrophobicity, poor stability and dispersibility in aqueous solutions, and poor drug loading [18, 19]. Thus, it is necessary to modify the nanocarriers with various polymers such as polyethylene glycol, chitosan, poly acrylic acid, and beta-cyclodextrin (βCD). It should be mentioned that βCD has appropriate properties such as being biodegradable and water-soluble improving stability, permeability, cyclic

structure and drug solubility. Furthermore, a selective and stable bond between biological guest molecules and cavities of βCD can be formed [20-23]. However, low drug release in human plasma is a critical issue. The introduction of thermosensitive polymers can be enhanced drug release [24]. Poly N-isopropylacrylamide polymer (PNIPAA) is an effective thermosensitive polymer showing a lower critical solution temperature (LCST) at around 32°C. To increase the LSCT and enhance the drug release, several monomers such as N, N-dimethyl acrylamide (DMAA) has been applied for copolymerization of PNIPAA[25]. In a study conducted by Xi et al., a thermo-sensitive polymer was prepared by copolymerization of NIPAA and DMAA with an LCST of 38.8°C in phosphate buffer saline (PBS) which was higher than LCST of NIPAA. Their results showed that a higher LCST in PBS leads to targeted drug delivery in tumor tissue with local hyperthermia [24]. Consequently, the modification of nanosheets as NIR-absorbing agents with appropriate polymers can be useful in drug delivery systems. Up to now, modification of metal sulfide nanosheets with βCD and copolymerized thermosensitive polymer has so far not been evaluated in drug delivery systems in the absence and presence of NIR laser.

In this research, two multifunctional NIPAA/βCD/WS_2 and NIPAA/DMAA/βCD/WS_2 nanocarriers were prepared for in vitro tamoxifen drug release in the absence and presence of a NIR laser. The characterization of the prepared nanocarriers was performed using XRD, FTIR, FE-SEM, and TGA analyses. The effect of temperature on tamoxifen drug release was evaluated at three different temperatures (25, 37, and 50°C) with pH 7.4 in the absence of a NIR laser. Furthermore, the effect of laser light with a power density of 1 W/cm^2 on tamoxifen drug release was studied for chemo-photothermal therapy. The release data were evaluated using kinetics models. The stability of the tamoxifen drug was also investigated.

Experimental

Materials

Tamoxifen drug was purchased from WOCKHARDT (UK). βCD was purchased from Seebio Co. in China. Tungsten disulfide (WS_2) was obtained from Sigma Aldrich. NIPAAP, DMAA, sodium hydroxide, methanol, hydrochloric acid, dimethylformamide, acetone, trichloro methane, ethanol and Azobisisobutyro nitrile were obtained from Merck. Furthermore, maleic anhydride was provided from Urokom Co. in China. Dialysis bag with a typical molecular weight cut-off: 14 kDa was purchased from Sigma Aldrich (USA).

βCD monomer preparation

To prepare the βCD monomer, at first, the specified amount of βCD (6.0 g) and maleic anhydride (2.5 g) was increased into 60 ml dimethylformamide under magnetic stirring at a temperature of 80°C for 10 h. The temperature of the resulting mixture decreased to the ambient temperature. Then, a white precipitate was formed after the addition of 50 ml trichloro methane to the mixture. The resulting precipitate was separated by filtration and washed with sufficient acetone and finally dried in an oven at a temperature of 50°C for three days.

Synthesis of NIPAA/βCD/WS_2 and NIPAA/DMAA/βCD/WS_2 nanocarriers

For the preparation of the NIPAA/βCD/WS_2 nanocarrier, at first, the specified amount of WS_2 (0.1 g), βCD monomer (0.7 g), and NIPAAP (1.0 g) were added into the specified ethanol (50 ml) under nitrogen atmosphere for ten min. It should be mentioned that Azobisisobutyro nitrile was used as an initiator. Thus, the specified amount of initiator (0.1 g) was added at a temperature of 65°C for 7 h. After cooling to ambient temperature, the obtained participate was separated by filtration and washed with sufficient distilled water, and then dried at a temperature of 50°C. Furthermore, NIPAA/DMAA/βCD/WS_2 nanocarrier was synthesized by using the same process with 1.0 g of NIPAA, 0.1 g of DMAA, 0.7 g of βCD monomer and 0.1 g of WS_2 nanosheet.

Tamoxifen loading onto the synthesized nanocarriers

Tamoxifen drug was loaded onto the NIPAA/βCD/WS_2 and NIPAA/DMAA/βCD/WS_2 nanocarriers using a batch adsorption process. The adsorption experiments were performed at ambient temperature, an adsorbent dosage of 1 g/l (0.01 g of the synthesized nanocarriers in 10 ml tamoxifen drug solution), contact time of 30 min, and an initial drug concentration of 20.0 mg/l. The amount of loaded tamoxifen drug was evaluated as follows [26, 27]:

$$q_e = \frac{(C_0 - C_e)\ \mathrm{V}}{m} \qquad (1)$$

where C_0 and C_e (mg/L) denote the initial and equilibrium concentration of tamoxifen drug, respectively; q_e (mg/g) denotes the amount of loaded tamoxifen drug; V (L) represents the volume of drug solution and m (g) denotes the mass of nanocarrier. Furthermore, a UV–vis spectrophotometer (perkin-lambda 25, USA) was applied to specify the final concentration of the tamoxifen drug.

Characterization investigations

The functional groups of the synthesized nanocarriers were specified using FTIR analysis (Spectrum Two, PerkinElmer Co). To determine the crystal structure of the synthesized nanocarriers, XRD analysis was used (X' Pert Pro, Panalytical Co). The shape and morphology of the synthesized nanocarriers were evaluated using FE-SEM analysis (ZEISS model SIGMA VP-500). Furthermore, the thermal stability of the synthesized nanocarriers was studied using TGA (Shimadzu co, Kyoto, Japan).

The photothermal effect of the synthesized nanocarriers

The photothermal effect of NIPAA/βCD/WS_2 and NIPAA/DMAA/βCD/WS_2 nanocarriers was investigated. The prepared suspensions containing 0.4 g of synthesized sample and 50 mL PBS solution (a ratio of 8 mg/mL or 800 μg/mL) were irradiated under NIR laser at 808 nm with a power density of 1.0 W/cm^2 for 5.0 min.It should be mentioned that the MDL-III-808nm laser was purchased from Changchun New Industries Optoelectronics Tech. Co. It was used to irradiate the samples. Then, the temperature of the suspensions was measured using a digital thermometer with a thermocouple probe (Pyrometer Co).

Release of tamoxifen drug in the absence and presence of NIR laser

The release of tamoxifen drug from the synthesized nanocarriers was studied in a simulated body system with pH 7.4 in the absence and presence of a NIR laser. The drug release experiments were performed using a dialysis method as follows. For experiments in the absence of a NIR laser, the specified amounts of NIPAA/βCD/WS_2-loaded tamoxifen and NIPAA/DMAA/βCD/WS_2-loaded tamoxifen samples were placed in the dialysis bag. The resulting dialysis bag was immersed in the specified amount of phosphate buffer solution (pH 7.4) and then put in a shaker at various temperatures (25-50°C) for 6 h. It should be mentioned that the release medium of phosphate-buffered saline (PBS) solution with pH 7.4 was prepared by dissolving 8.00 g NaCl, 0.19 g KH_2PO_4 and 2.38 g Na_2HPO_4(Aldrich) in 1L distilled water. The ratio of the sample to PBS solution was 1 mg/mL. The specified amount of floating solution (3.0 mL) was sampled at distinct intervals and 3.0 mL of fresh buffer solution was substituted to fix the volume of the drug release medium. The release experiments in the presence of NIR laser irradiation were performed at 808 nm (1.0 W/cm^2; 5.0 min). The released tamoxifen from the synthesized nanocarriers was sampled before NIR laser irradiation at the specified interval times. The released tamoxifen was determined using a UV-vis spectrophotometer.

Investigation of tamoxifen release kinetic

The kinetics modeling of drug release can be applied to evaluate the drug release mechanism from the nanocarriers. To investigate the mechanism of tamoxifen release from the NIPAA/βCD/WS_2 and NIPAA/DMAA/βCD/WS_2 nanocarriers in the absence and presence of NIR laser, the experimental release data were investigated using some relevant kinetic models including Zero-order, First-order, Higuchi and Ritger-Peppas models which are given as follows [28-31]:

Zero-order model: $$Q_t = k_0 t \quad (2)$$

First-order model: $$Q_t = 1 - \exp\left(k_1' t\right) \quad (3)$$

Higuchi model: $$Q_t = k_H t^{0.5} \quad (4)$$

Ritger-Peppas model: $$Q_t = k_{RP} t^n \quad (5)$$

where Q_t represents the fraction of tamoxifen released at time t; k_0, k_1', k_H, and k_{RP} denote the release constants of zero-order, first-order, Higuchi, and Ritger-Peppas kinetic models, respectively; and n denotes the release exponent indicating the transport mechanism. A Fickian diffusion in the drug release process is dominant for n ≤0.5. A non-Fickian transport containing both diffusion and case II transport (relaxation and degradation) is dominant for 0. 5<n<1.0; and only the case II transport mechanism is dominant for n=1 (zero-order kinetic model) [28, 31, 32].

Evaluation of drug stability

The stability evaluation of the tamoxifen drug loaded on the synthesized NIPAA/βCD/WS_2 and NIPAA/DMAA/βCD/WS_2 nanocarriers was performed at various temperatures (25-55°C) at environmental humidity. The prepared batches of formulations were placed in glass vials and put at the specified accelerated temperatures. The resulting samples were evaluated at regular intervals of 0.0, 1.0, 2.0, and 3.0 months. A UV–vis spectrophotometer was used to analyze the tamoxifen content. To investigate the degradation kinetics and shelf life of each formulation, the contents of the degraded tamoxifen drug and the contents of the remaining tamoxifen drug at each time were determined. Several mathematical relationships were used to determine the degradation kinetic parameters including degradation rate constant, shelf life, and activation energy. The degradation

rate constant (K) was estimated at each temperature using the first-order degradation kinetic model which is given by the following equation [33, 34].

First order degradation model: $$Log[A]=\text{Log}[A_0]-\frac{K}{2.303}\ t \quad (6)$$

where K (1/month) denotes the degradation rate constant; $[A_0]$is the % remaining tamoxifen at the initial time and [A] denotes the % remaining tamoxifen at time t. The K value at each temperature can be estimated from the slope of Eq. (6). The shelf life ($T_{0.9}$) is the time needed for degradation of 10% tamoxifen drug which can be determined as follows [33]:

$$T_{0.9}=\frac{0.1052}{K_{25}} \quad (7)$$

where K_{25} denotes the degradation rate constant at a temperature of 25°C.

To estimate the activation energy (E_a), the linear form of the Arrhenius plot was used [33, 34]. It is given as follows:

$$Log(K)=Log(A)-\frac{E_a}{2.303\ R}\times\frac{1}{T} \quad (8)$$

where A is the pre-exponential constant which can be estimated from the intercept of the line of the Arrhenius equation; E_a is the activation energy which can be estimated from the slope of the line of the Arrhenius equation; R is the universal gas constant and T is the absolute temperature (K).

Results and discussion

Characterization study

The XRD analysis was applied to identify the crystal phases of WS_2, NIPAA/βCD/WS_2, and NIPAA/DMAA/βCD/WS_2 nanocarriers. Figure 1 shows the XRD patterns of the samples. According to JCPDS Card number 032-1626, the five diffraction peaks of the WS_2 nanosheet were located at 2θ= 14.2° (002), 28.7° (100), 33.4° (011), 39.4° (013) and 50.3° (105) [35, 36]. As observed, a strong diffraction peak with a lattice plane of (002) was observed for the WS_2 nanosheet presented in the structure of all samples. However, the intensity of other peaks was weak showing that exfoliated WS_2 had a mono-layered or few-layered structure [37]. Furthermore, the XRD diffraction peaks of samples did not change significantly after modification of WS_2 with the applied polymers confirming the preservation of WS_2 crystals in the structure of the samples. However, a slight reduction in the intensity of peaks can be due to the WS_2 coverage with the applied polymers.

The functional groups of NIPAA/βCD/WS_2, NIPAA/DMAA/βCD/WS_2, NIPAA/βCD/WS_2-tamoxifen, and NIPAA/DMAA/βCD/WS_2-tamoxifen samples were evaluated using FTIR (Figure

2). As shown, the corresponding peak of sulfur was observed at about 483 cm^{-1} for NIPAA/βCD/WS_2 and 480 cm^{-1} for NIPAA/DMAA/βCD/WS_2 sample. Also, W-S and S-S bonds were recognized at about 609 cm^{-1} and 1157 cm^{-1} for NIPAA/βCD/WS_2 and 601 cm^{-1} and 1158 cm^{-1} for NIPAA/DMAA/βCD/WS_2 sample, respectively [35].

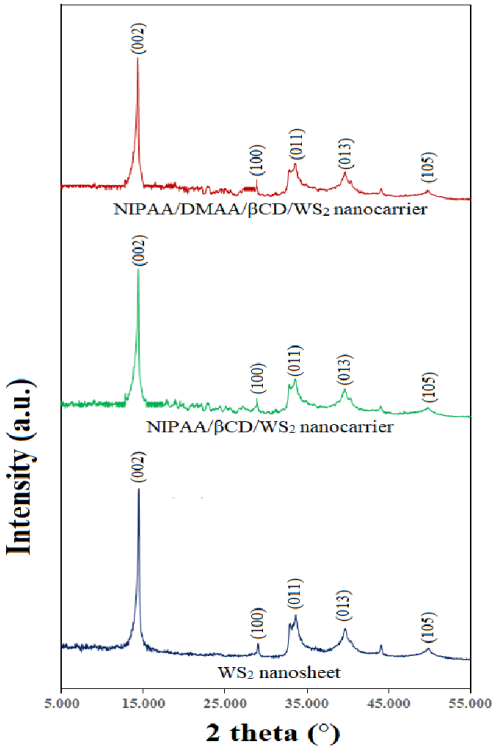

Figure 1. The XRD patterns of the WS_2, NIPAA/βCD/WS_2, and NIPAA/DMAA/βCD/WS_2 nanocarriers.

This showed the presence of WS_2 nanosheet in the structure of both samples. A peak that appeared at 3414 cm^{-1} is attributed to the -OH bonds. For all samples, the C-O stretching vibration of glucose units of βCD was observed at about 1000-1300 cm^{-1}. The mentioned peaks confirmed the presence of βCD polymer in the structure of both samples. For NIPAA/βCD/WS_2 sample, the peaks observed at 1637 cm^{-1} and 1712 cm^{-1} are related to the C=O amide vibrations and C=C vibrations of the applied polymer, respectively. Furthermore, the peak at 2926 cm^{-1} is attributed to the C-H stretching vibrations [24, 38, 39]. The presence of n-isopropyl acrylamide was confirmed by the peaks at 1637 cm^{-1} and a weak peak at 3241 cm^{-1} attributing to the amide and N-H groups, respectively. For NIPAA/DMAA/βCD/WS_2 sample, the peaks at 1031, 1342, 1392 and 1662, and 2929 cm^{-1} are assigned to the C-CH_3, C-N, N-CH_3, the C=O (carbonyl) stretching of amide compounds confirming the existence of N, N-dimethyl acrylamide in the structure of NIPAA/DMAA/βCD/WS_2

sample [24, 40, 41]. For all samples, a broad peak at 3400-3500 cm^{-1} is assigned to the –OH stretching vibration [40, 41]. It was found that the FTIR spectrum of samples before tamoxifen loading was similar to that after tamoxifen loading. This confirmed that the structure of the synthesized samples was preserved after the absorption of tamoxifen.

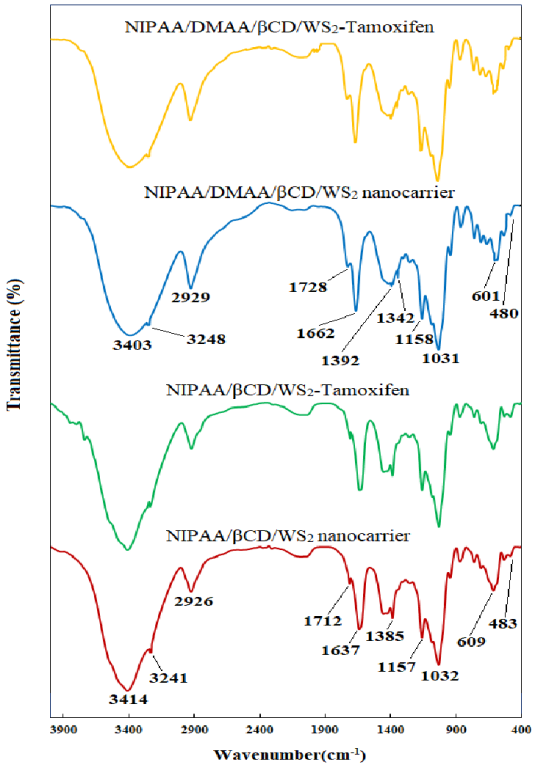

Figure 2. The FTIR analysis NIPAA/βCD/WS_2, NIPAA/DMAA/βCD/WS_2, NIPAA/βCD/WS_2-tamoxifen and NIPAA/DMAA/βCD/WS_2-tamoxifen samples.

The FESEM analysis was used to study the microstructure and morphology of NIPAA/βCD/WS_2 and NIPAA/DMAA/βCD/WS_2 nanocarriers (Figure 3). As shown, both samples had a flake shape and layered structure due to the presence of WS_2 nanosheets. It should be mentioned that the structure of nanosheets is nonuniform. The width and length of nanosheets lay between 50 nm and 600 nm. Similar shapes were observed by others [42].

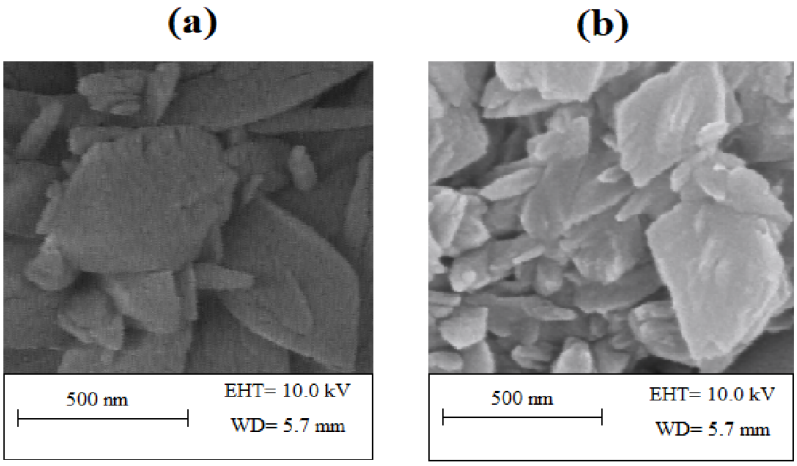

Figure 3. The FESEM analysis of (a) NIPAA/βCD/WS_2 and (b) NIPAA/DMAA/βCD/WS_2 nanocarriers.

Comparison of Figure 3 a with b depicted that the structure of both samples was similar to a layered structure. This showed that the layered structure of the NIPAA/DMAA/βCD/WS_2 nanocarrier was preserved after modification with DMAA. Thermogravimetry has been applied to evaluate the thermal stability and decomposition mechanism of many samples. In this study, TGA was used to analyze the thermal stability of WS_2 NIPAA/βCD/WS_2 and NIPAA/DMAA/βCD/WS_2 nanocarriers. The results of TGA displayed that WS_2 sample had a small weight loss (2.7%) in the temperature range lower than 150°C which can be due to the water evaporation from the surface of samples. The weight of WS_2 sample was fixed after 150°C and no weight loss was observed. The weight loss of NIPAA/βCD/WS_2 and NIPAA/DMAA/βCD/WS_2 nanocarriers in this step were 7.8% and 8.0%, respectively which can be due to the elimination of water adsorbed on the surface of nanocarriers and located in the cavity of βCD.

Similar observations were attained by other researchers [43, 44]. The pyrolysis of samples indicated a second weight loss of 41.6% for NIPAA/βCD/WS_2 nanocarrier at 290°C and 34.3% for NIPAA/DMAA/βCD/WS_2 nanocarrier at 305°C. This reduction can be due to the glucose melting of βCD structure and decomposition of NIPAA and DMAA polymers [43-45]. The final stage of degradation occurred at 390°C and 405°C for NIPAA/βCD/WS_2 (10.5%) and NIPAA/DMAA/βCD/WS_2 (9.1%) nanocarriers, respectively. This can be due to the decomposition of glucose and breakage of βCD, NIPAA, and DMAA structures [44]. The overall weight loss of NIPAA/βCD/WS_2 and NIPAA/DMAA/βCD/WS_2 nanocarriers was found to be 59.9% and 51.4%, respectively. This displayed that the thermal stability of NIPAA/DMAA/βCD/WS_2 was higher than that of NIPAA/βCD/WS_2 sample. This can be due to the addition of DMAA in the copolymer chain of NIPAA/DMAA/βCD/WS_2 sample (polymerization of NIPAA with DMAA) [45].

The photothermal effect of the synthesized nanocarriers in the presence of NIR laser

The photothermal property of NIPAA/βCD/WS_2 and NIPAA/DMAA/βCD/WS_2 dispersions in PBS solution was investigated using NIR laser at 808 nm with a power density of 1.0 W/cm^2 for 5.0 min. In this study, PBS solution was applied as a blank dispersion. Figure 4 shows the photothermal performance of blank, NIPAA/βCD/WS_2 and NIPAA/DMAA/βCD/WS_2 dispersions in the presence of NIR laser.

As shown, the temperature of NIPAA/βCD/WS_2 and NIPAA/DMAA/βCD/WS_2 solutions increased significantly during the irradiation for 5 min, whereas the PBS solution temperature did not change significantly. The temperature increase (ΔT(°C)) of blank, NIPAA/βCD/WS_2, and NIPAA/DMAA/βCD/WS_2 dispersions were found to be 3.2, 37.1, and 46.0 °C, respectively. The higher heat generation efficiency of NIPAA/βCD/WS_2 and NIPAA/DMAA/βCD/WS_2 dispersions may be due to the presence of WS_2 nanosheet in their structure. It should be mentioned that WS_2 nanosheets can be used as NIR absorbing agents in drug delivery systems because of the high surface area, small band gap, and high NIR absorbance for effective hyperthermia generation under laser light [13, 16, 17]. Furthermore, the heat generation efficiency of NIPAA/DMAA/βCD/WS_2 dispersion was greater than that of NIPAA/βCD/WS_2 dispersion. This showed that the heat generation efficiency increased after DMAA addition in the structure of NIPAA/βCD/WS2 sample. Thus, DMAA has an important role. The copolymerization of NIPAA and DMAA and also insertion of thermo-sensitive polymer chains with WS_2 nanosheet led to an improvement in the absorption of NIR light and heat generation efficiency [24].

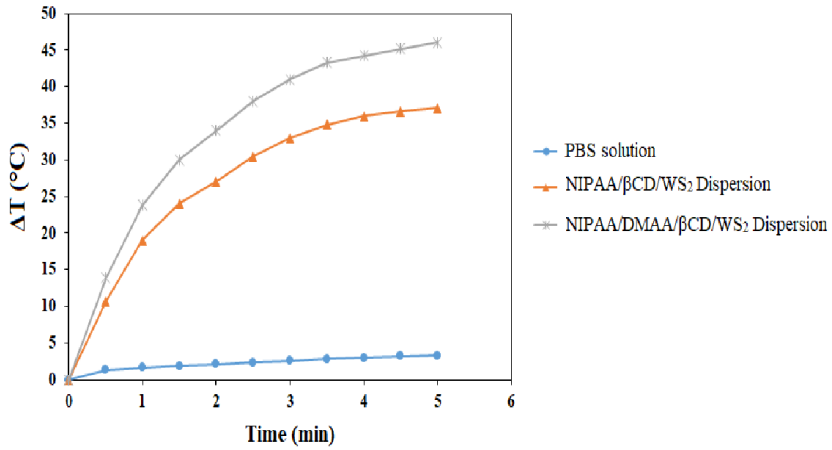

Figure 4. The photothermal performance of blank, NIPAA/βCD/WS_2 and NIPAA/DMAA/βCD/WS_2 dispersions in the presence of NIR laser.

Tamoxifen drug release in the absence and presence of NIR laser

Tamoxifen release from NIPAA/βCD/WS_2 and NIPAA/DMAA/βCD/WS_2 samples was studied in a simulated body system with pH 7.4 in the absence of NIR laser at various release temperatures (25-50°C). The effect of temperature on the tamoxifen release from NIPAA/βCD/WS_2 and NIPAA/DMAA/βCD/WS_2 samples at various release temperatures is indicated in Figure 5. As shown, tamoxifen release increased with the increase in temperature for all samples. Tamoxifen release was favored at higher temperatures (50°C) compared to 25 and 37°C. The higher tamoxifen release at higher temperatures can be attributed to the properties of applied thermosensitive polymers.

The thermosensitive polymer of NIPAA/βCD/WS_2 sample was NIPAA with a LCST of about 33°C [46]. For NIPAA/DMAA/βCD/WS_2 sample, the LCST increased by copolymerization of NIPAA and DMAA monomer. So, the DMAA incorporation leads to the increase of LCST [24]. The LCST of NIPAA/DMAA copolymer was about 38.8 °C. At temperatures lower than LCST, the blocks are hydrophilic and the release of the tamoxifen drug was conducted from a hydrophobic core a portion of tamoxifen remained in the cores of micelles because the samples had a hydrophobic/hydrophilic structure and the blocks could stabilize the tamoxifen drug in micellar cores [47]. Thus, a lower tamoxifen release from both synthesized samples was observed at 25°C because this temperature was lower than LCST. But, the arms of NIPAA polymer and NIPAA/DMAA copolymer turned out to be hydrophobic at temperatures greater than LCST, and the drug release had two steps including (1) a slow release of tamoxifen from the hydrophobic core to the hydrophobic shell (NIPAA polymer and NIPAA/DMAA copolymer) and (2) a fast release of tamoxifen that transferred on the hydrophobic shell (NIPAA polymer and NIPAA/DMAA copolymer) to the medium of tamoxifen drug release [46]. As shown, the drug release of tamoxifen from the NIPAA/βCD/WS_2 sample at 37°C was greater than that from NIPAA/DMAA/βCD/WS_2 sample because this temperature was greater than the LCST of NIPAA thermosensitive polymer (33°C) and lower than LCST of NIPAA/DMAA thermosensitive polymer (38.8 °C). Also, a higher tamoxifen release from both synthesized samples was observed at 50°C compared to other temperatures because this temperature was greater than the LCST of NIPAA polymer and NIPAA/DMAA copolymer. It was found that thermosensitive polymers play a key role in drug release. Moreover, the release of tamoxifen drug from both samples increased during the time at a constant temperature. The release of tamoxifen from the synthesized samples during the time can be due to the weakening of hydrogen bonds between tamoxifen and the synthesized samples [48].

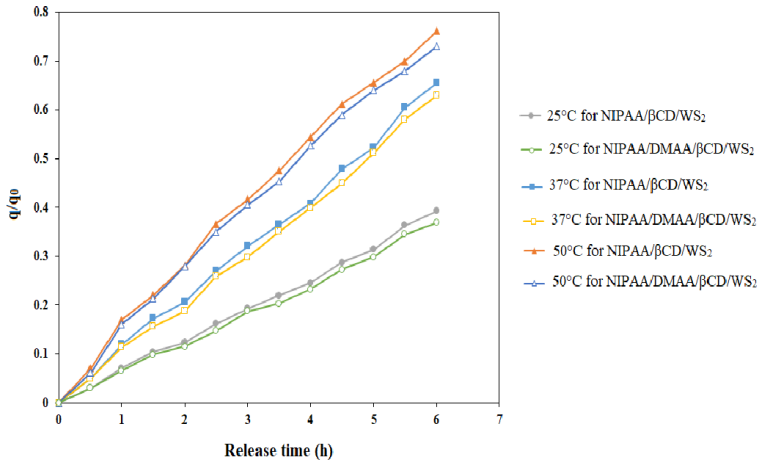

Figure 5. The effect of temperature on the tamoxifen release from the synthesized NIPAA/βCD/WS_2 and NIPAA/DMAA/βCD/WS_2 samples in the presence of NIR laser in a simulated body system with pH 7.4.

Also, tamoxifen release from NIPAA/βCD/WS_2 and NIPAA/DMAA/βCD/WS_2 samples were evaluated in a simulated body system with pH 7.4 at 37°C in the presence of NIR laser (Figure 6). As observed, the tamoxifen release from both synthesized samples with NIR laser was greater than that without NIR laser. Thus, a higher tamoxifen release with NIR laser irradiation was observed. This indicated that the irradiation of NIR laser led to the generation of a higher temperature than LCST of samples, and a higher drug release occurred [47]. Furthermore, a higher drug release from NIPAA/DMAA/βCD/WS_2 sample in the presence of NIR laser was observed compared to NIPAA/βCD/WS_2 sample. Indeed, the higher drugs are released from thermosensitive polymer with an increase in temperature and heat generation efficiency by NIR laser [47]. Thus, the higher heat generation efficiency of NIPAA/DMAA/βCD/WS_2 sample led to an increase in drug release. As mentioned, the higher heat generation of NIPAA/DMAA/βCD/WS_2 can be due to the copolymerization of NIPAA and DMAA and also the insertion of thermo-sensitive polymer chains with WS_2 nanosheet leading to an increase in absorption of NIR light [24].

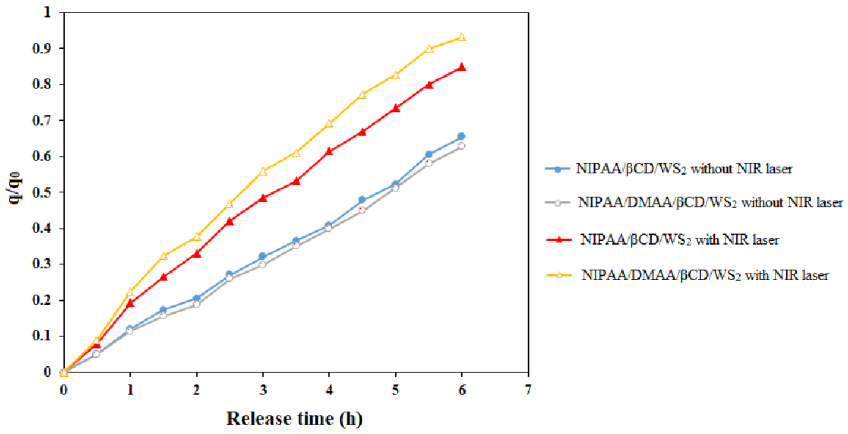

Figure 6. Tamoxifen release from the synthesized NIPAA/βCD/WS_2 and NIPAA/DMAA/βCD/WS_2 samples in the presence of NIR laser in a simulated body system with pH 7.4 at 37°C.

Investigation of release kinetics in the absence and presence of NIR laser

To study the mechanism of tamoxifen release from the synthesized NIPAA/βCD/WS_2 and NIPAA/DMAA/βCD/WS_2 nanocarriers in the absence and presence of NIR laser irradiation, Zero-order, First-order, Higuchi and Ritger-Peppas kinetic models were used. Table 1 indicates the release kinetic parameters of the tamoxifen drug at different temperatures in the absence of NIR laser. Also, Table 2 shows the release kinetic parameters of tamoxifen drug from the synthesized NIPAA/βCD/WS_2 and NIPAA/DMAA/βCD/WS_2 nanocarriers in the absence and presence of NIR laser at 37°C. The results showed that the experimental data were corroborated with the zero-order kinetic model according to the R^2 value. As observed, the highest R^2 value with and without NIR laser was obtained for the zero-order model. This displayed that only the case II transport mechanism was dominant (n=1 for the zero-order kinetic model). The mechanism of drug release in the case II transport mechanism includes the relaxation of polymeric chains or swelling [49, 50]. Indeed, the polymer begins to swell and no drug diffusion takes place through the polymer phase. The swelling of polymers occurs in the gelled region while polymer relaxation occurs on the gel-vitreous polymeric interface. There is no solvent and tamoxifen diffusion through the vitreous region. After the penetration process through the gelled region with the polymer cleavage, the glass transition temperature of a polymer is reduced and the relaxation process occurs [50, 51]. The swelling of polymers that existed in the structure of NIPAA/βCD/WS_2 and NIPAA/DMAA/βCD/WS_2 nanocarriers (solvent diffusion through the samples) is very fast compared to the relaxation process. Also, the n values (diffusion exponent) obtained from the Ritger-Peppas model were close to one (Table 1) confirming the mechanism of case II transport.

Table 1. The release kinetic parameters of tamoxifen drug from the synthesized NIPAA/βCD/WS_2 and NIPAA/DMAA/βCD/WS_2 nanocarriers at different temperatures in the absence of NIR laser.

sample	Temperature(°C)	Zero order model		
		K_0	R^2	
NIPAA/βCD/WS_2	25	0.064	0.999	
	37	0.107	0.999	
	50	0.133	0.998	
NIPAA/DMAA/βCD/WS_2	25	0.061	0.999	
	37	0.103	0.999	
	50	0.128	0.998	
		First order model		
		K'_1	R^2	
NIPAA/βCD/WS_2	25	0.077	0.975	
	37	0.152	0.973	
	50	0.210	0.980	
NIPAA/DMAA/βCD/WS_2	25	0.072	0.995	
	37	0.143	0.984	
	50	0.198	0.993	
		Higuchi model		
		k_H	R^2	
NIPAA/βCD/WS_2	25	0.128	0.959	
	37	0.214	0.959	
	50	0.267	0.964	
NIPAA/DMAA/βCD/WS_2	25	0.121	0.958	
	37	0.205	0.956	
	50	0.259	0.974	
		Ritger-Peppas model		
		K_{RP}	n	R^2
NIPAA/βCD/WS_2	25	0.065	0.992	0.995
	37	0.108	0.991	0.995
	50	0.149	0.926	0.993
NIPAA/DMAA/βCD/WS_2	25	0.062	0.987	0.996
	37	0.103	0.993	0.995
	50	0.139	0.958	0.990

Furthermore, the rate constant estimated for both synthesized samples in the absence of a NIR laser showed that a higher drug release rate was obtained at a higher temperature due to the higher K value (Table 1). The higher K value in the presence of a NIR laser confirmed that the tamoxifen release rate in the presence of a laser was greater than that in the absence of a laser (Table 1).

Table 2. The release kinetic parameters of tamoxifen drug from the synthesized NIPAA/βCD/WS_2 and NIPAA/DMAA/βCD/WS_2 nanocarriers in the absence and presence of NIR laser at 37°C.

Sample	NIR laser	Zero order model	
		K_0	R^2
NIPAA/βCD/WS_2	No	0.107	0.999
	Yes	0.150	0.997
NIPAA/DMAA/βCD/WS_2	No	0.103	0.999
	Yes	0.169	0.995
		First order model	

			K'_1	R^2
NIPAA/βCD/WS_2	No		0.152	0.973
	Yes		0.266	0.981
NIPAA/DMAA/βCD/WS_2	No		0.143	0.984
	Yes		0.359	0.962
			Higuchi model	
			k_H	R^2
NIPAA/βCD/WS_2	No		0.214	0.959
	Yes		0303	0.978
NIPAA/DMAA/βCD/WS_2	No		0.205	0.956
	Yes		0.342	0.981
			Ritger-Peppas model	
		K_{RP}	n	R^2
NIPAA/βCD/WS_2	No	0.108	0.991	0.995
	Yes	0.173	0.915	0.991
NIPAA/DMAA/βCD/WS_2	No	0.103	0.993	0.995
	Yes	0.199	0.901	0.987

The zero-order kinetic model at different temperatures in the absence of NIR laser for tamoxifen release from both synthesized samples is shown in Figure 7 and the zero-order kinetic model at 37°C in the presence of NIR laser for tamoxifen release from both synthesized samples is shown in Figure 8.

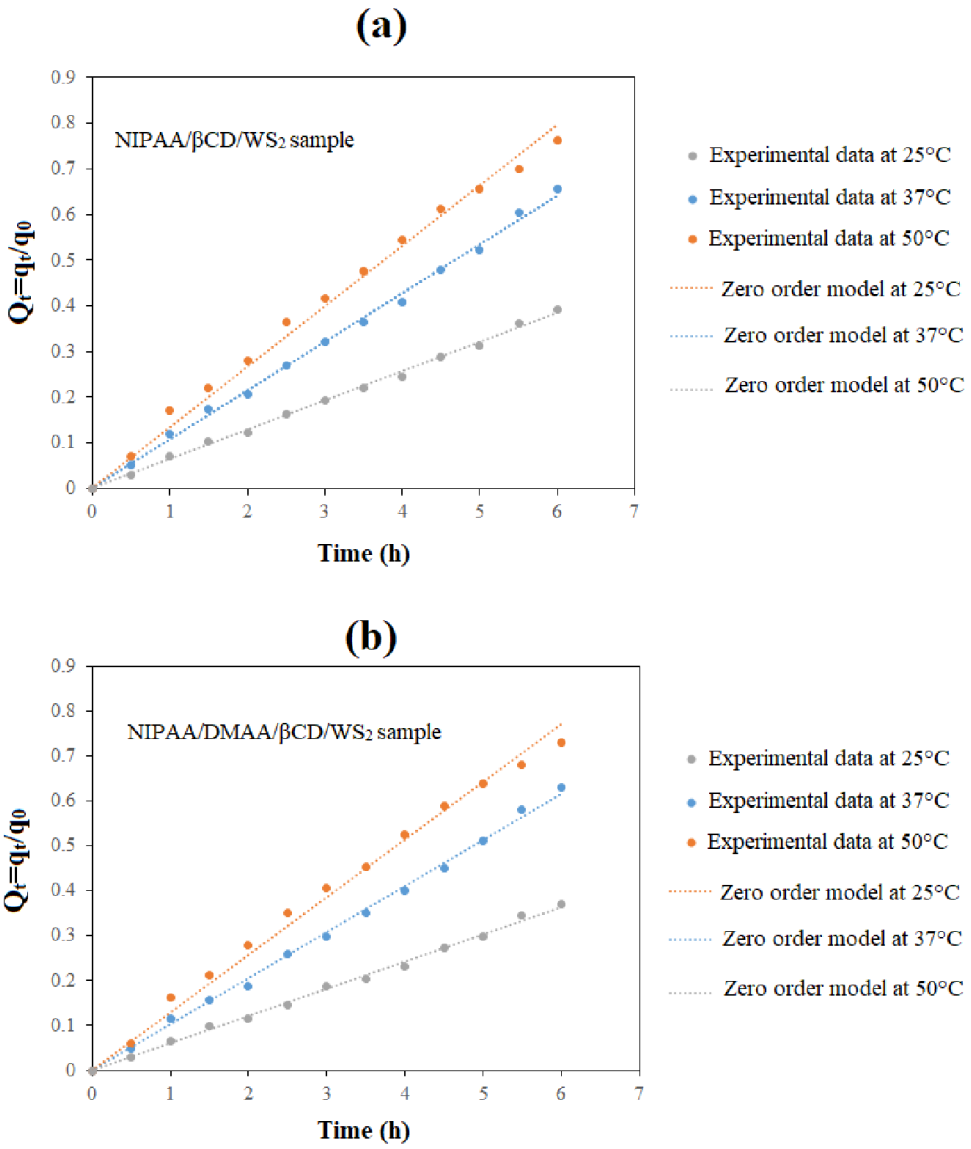

Figure 7. The zero-order kinetic model at different temperatures in the absence of NIR laser for tamoxifen release from (a) NIPAA/βCD/WS_2 and (b) NIPAA/DMAA/βCD/WS_2samples.

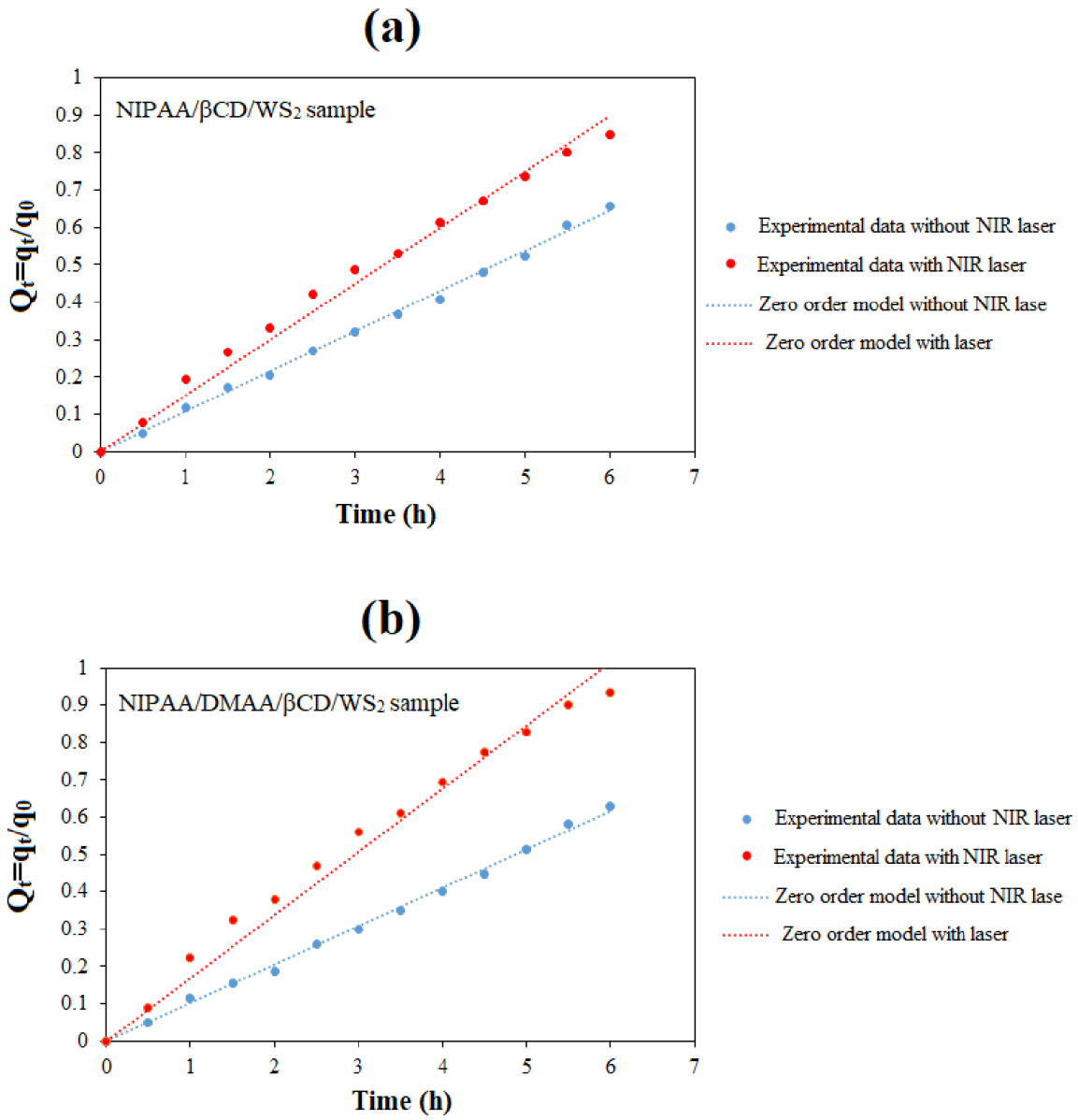

Figure 8. The zero-order kinetic models at 37°C in the presence of NIR laser for tamoxifen release from (a) NIPAA/βCD/WS_2 and (b) NIPAA/DMAA/βCD/WS_2samples.

Evaluation of drug stability

There are different methods to investigate the stability of drugs. In this research, the accelerated storage stability was applied under distinct conditions of storage such as temperature and time of storage to evaluate the stability of tamoxifen drug loaded on the synthesized NIPAA/βCD/WS_2 and NIPAA/DMAA/βCD/WS_2 nanocarriers. Table 3 indicates the % remained and degraded content of tamoxifen loaded on both nanocarriers at each time for different storage temperatures. As shown, the degradation rate of tamoxifen was very slow for both nanocarriers confirming the suitable stability of tamoxifen drug during the accelerated storage tests after 3 months. As mentioned, the

first-order degradation kinetic model and Arrhenius equation were applied to estimate the degradation rate constant and activation energy. According to the estimated values of K and E_a, the shelf life and stability of tamoxifen were evaluated.

Table 3. percentage of Degraded and remained tamoxifen drug loaded on both nanocarriers at intervals of 0, 1, 2, and 3 months at various storage temperatures.

Time (month)	Temperature (°C)	For NIPAA/βCD/WS_2		For NIPAA/DMAA/βCD/WS_2	
		% Degraded concentration (mg/L)	% Remained concentration (mg/L)	% Degraded concentration (mg/L)	% Remained concentration (mg/L)
0	25	0.00	100.00	0.00	100.00
1		0.35	99.65	0.31	99.69
2		0.73	99.27	0.64	99.36
3		1.19	98.81	1.12	98.88
0	35	0.00	100.00	0.00	100.00
1		0.58	99.42	0.53	99.47
2		1.16	98.84	1.08	98.92
3		1.87	98.13	1.81	98.19
0	45	0.00	100.00	0.00	100.00
1		1.70	98.30	1.62	98.38
2		3.61	96.39	3.51	96.49
3		5.19	94.81	5.04	94.96
0	55	0.00	100.00	0.00	100.00
1		1.90	98.10	1.79	98.21
2		4.00	96.00	3.76	96.24
3		6.41	93.59	6.07	93.93

Thus, the kineticsof first order degradation model is illustrated for both synthesized NIPAA/βCD/WS_2 and NIPAA/DMAA/βCD/WS_2 nanocarriers at different temperatures (Figure 9). The K values were estimated from the slope of the line at each temperature for both NIPAA/βCD/WS_2-tamoxifen and NIPAA/DMAA/βCD/WS_2-tamoxifen samples which are given in Table 4. As observed, K values of NIPAA/DMAA/βCD/WS_2-tamoxifen sample at each temperature werelower than those of NIPAA/βCD/WS_2-tamoxifen. Also, shelf life ($T_{0.9}$) of tamoxifen was estimated to be 26.4 month□2.2 years for NIPAA/βCD/WS_2-tamoxifen and 28.4 month□2.4 years for NIPAA/DMAA/βCD/WS_2-tamoxifen sample.

Table 4. The K values were estimated from the first-order degradation model at each temperature for both NIPAA/βCD/WS_2-tamoxifen and NIPAA/DMAA/βCD/WS_2-tamoxifen samples.

Sample	Absolute temperature (K)	K (1/month)
NIPAA/βCD/WS_2	298	3.99×10^{-3}
	308	6.23×10^{-3}
	318	17.96×10^{-3}
	328	22.04×10^{-3}
NIPAA/DMAA/βCD/WS_2	298	3.70×10^{-3}
	308	6.03×10^{-3}
	318	17.46×10^{-3}
	328	20.82×10^{-3}

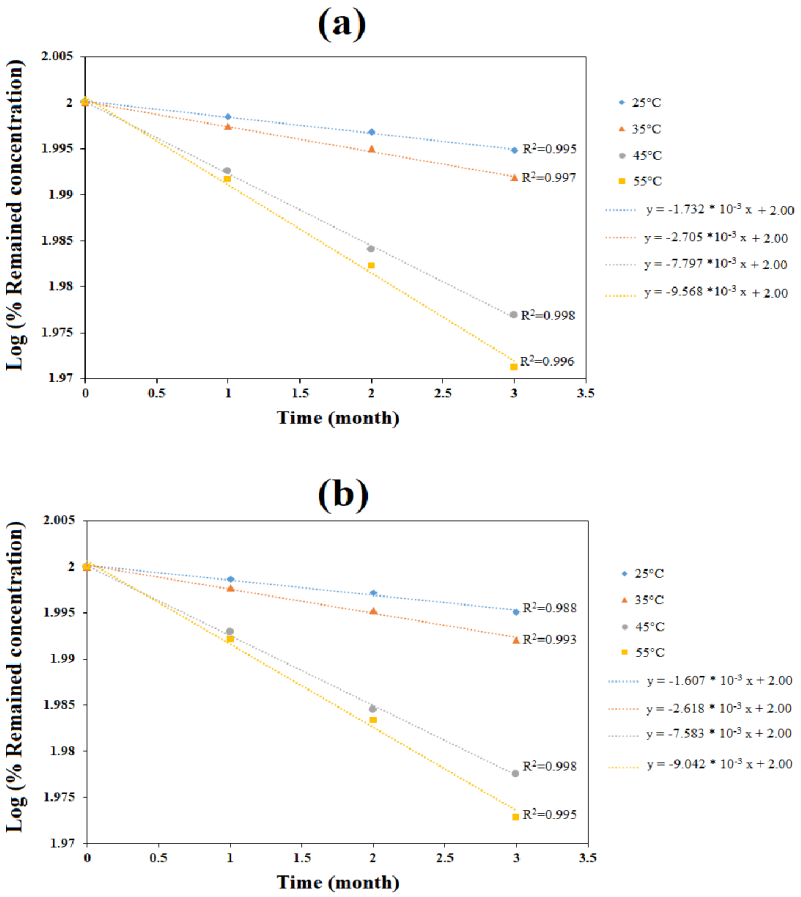

Figure 9. The kinetics of first order degradation model at different temperatures for (a) NIPAA/βCD/WS_2 and (b) NIPAA/DMAA/βCD/WS_2 nanocarriers.

This showed that the tamoxifen drug had high stability for both samples confirming that both synthesized nanocarriers are strong and stable materials and that there is a limitation for the movement of tamoxifen. However, the stability of tamoxifen loaded on NIPAA/DMAA/βCD/WS_2 nanocarrier was greater than the tamoxifen stability loaded on NIPAA/βCD/WS_2 nanocarrier due to the lower K values and higher shelf life. The activation energy of tamoxifen for both nanocarriers was determined according to Arrhenius linear plot. The E_a value was estimated to be 50.36 kJ/mol

for NIPAA/βCD/WS_2-tamoxifen and 50.88 kJ/mol for NIPAA/DMAA/βCD/WS_2-tamoxifen sample. These estimated values were almost close to the values of activation energy reported in the literature for tamoxifen drugs [33]. The higher tamoxifen activation energy for NIPAA/DMAA/βCD/WS_2 showed higher tamoxifen stability compared to NIPAA/βCD/WS_2.

Conclusion

Two novel NIPAA/βCD/WS_2 and NIPAA/DMAA/βCD/WS_2 nanocarriers were prepared for in vitro tamoxifen drug release in the absence and presence of NIR laser. The characterization of the prepared nanocarriers was performed using XRD, FTIR, FE-SEM, and TGA analyses. The FTIR results indicated that the structure of NIPAA/βCD/WS_2 and NIPAA/DMAA/βCD/WS_2 nanocarriers was maintained after the adsorption of tamoxifen. The results of FESEM showed that both samples had a flake shape and layered structure. The XRD analysis displayed distinct diffraction peaks of WS_2 nanosheet in the structure of both samples. The photothermal performance of samples was investigated using NIR laser. The results showed that the heat generation efficiency of NIPAA/DMAA/βCD/WS_2 dispersion was greater than that of NIPAA/βCD/WS_2 dispersion. The investigation of tamoxifen release from the samples was performed in a simulated body system with pH 7.4. Tamoxifen release in the absence of NIR laser was favored at higher temperatures (50°C) compared to 25 and 37°C. Also, the results displayed that tamoxifen release in the presence of NIR laser was greater than tamoxifen release in the absence of NIR laser. Also, a higher drug release from NIPAA/DMAA/βCD/WS_2 sample in the presence of NIR laser was observed compared to NIPAA/βCD/WS_2 sample. The results of release kinetics with and without NIR laser showed that the experimental data were corroborated with the zero-order kinetic model. The shelf life of tamoxifen was estimated to be 2.2 years for NIPAA/βCD/WS_2-tamoxifen and 2.4 years for NIPAA/DMAA/βCD/WS_2-tamoxifen sample. Thus, high stability of the tamoxifen drug was observed for both samples.

Acknowledgment

The authors gratefully acknowledge the support of Islamic Azad University, Central Tehran Branch (Iran).

References

[1]Z. Kazemi, F. Marahel, T. Hamoule, B. M. Goodajdar, *J. Appl. Chem. Res.,* 16, 30 (2022).

[2]W. Zhang, Z. Guo, D. Huang, Z. Liu, X. Guo, H. Zhong, *Biomater.,*32, 8555 (2011).

[3] S.K. Misra, P. Kondaiah, S. Bhattacharya, C. Rao, *Small,* 8, 131 (2012).

[4] S. A. Nazarali, S. A. Narod, *Breast Cancer: Targets and Therapy,* 6, 29 (2014).

[5]R. Abou-Jawde, T. Choueiri, C. Alemany, T. Mekhail, *Clinical Therapeutics,*25, 2121 (2003).

[6]N. Shahabadi, M. Razlansari, A. Khorshidi, H. Zhaleh, *Res. Chem. Intermed.,*46, 4257 (2020).

[7]S.M. Taimoory, A. Rahdar, M. Aliahmad, F. Sadeghfar, M.R. Hajinezhad, M. Jahantigh, P. Shahbazi, J.F. Trant, *J. Molec. Liq.,* 265, 96 (2018).

[8]T. Arimidex,*The Lancet Oncology,*7, 633 (2006).

[9]L. Li, W.-W. Yang, D.-G. Xu, *J.Drug Target.,*27, 423 (2019).

[10]A. Ramazani, M. Abrvash, S. Sadighian, K. Rostamizadeh, M. Fathi, *Res. Chem. Intermed.,*44, 7891 (2018).

[11]F. Bani, M. Adeli, S. Movahedi, M. Sadeghizadeh,*RSC Adv.,*6, 61141 (2016).

[12]M. Abbasian, F. Mahmoodzadeh, R. Salehi, A. Amirshaghaghi, *New J. Chem.,*41, 12777 (2017).

[13]Y. Liu, X. Ji, J. Liu, W.W. Tong, D. Askhatova, J. Shi, *Adv.Funct.Mater.,*27, 1703261 (2017).

[14]D. Luo, K.A. Carter, D. Miranda, J.F. Lovell, *Adv. Sci.,* 4, 1600106 (2017).

[15]K. Yang, J. Wan, S. Zhang, B. Tian, Y. Zhang, Z. Liu, *Biomater.,*33, 2206 (2012).

[16]S. Wang, X. Li, Y. Chen, X. Cai, H. Yao, W. Gao, Y. Zheng, X. An, J. Shi, H. Chen, *Adv.Mater.,*27, 2775 (2015).

[17]W. Yin, L. Yan, J. Yu, G. Tian, L. Zhou, X. Zheng, X. Zhang, Y. Yong, J. Li, Z. Gu,*ACS Nano,*8, 6922 (2014).

[18]M. Khafaji, M. Zamani, M. Golizadeh, O. Bavi, *Biophys.Rev.,*11, 335 (2019).

[19]W.Z. Teo, E.L.K. Chng, Z. Sofer, M. Pumera, *Chem. A Eur. J.,*20, 9627 (2014).

[20]R. Freeman, T. Finder, L. Bahshi, I. Willner, *Nano Lett.,*9, 2073 (2009).

[21]M. Messner, S.V. Kurkov, P. Jansook, T. Loftsson, *Inter.J.Pharmaceutics,*387, 199 (2010).

[22]S. Prabu, R. Rajamohan, K. Sivakumar, S. Mohamad, *Polycom. Arom. Comp.*,41, 992 (2021).

[23]M.V. Rekharsky, Y. Inoue, *Chem.Rev.,*98, 1875 (1998).

[24]L. Xi, C. Li, Y. Wang, Y. Gong, F. Su, and S. Li, *J. Pharmaceutical Sci.,*109, 2544 (2020).

[25]H. Tian, Z. Tang, X. Zhuang, X. Chen, X. Jing, *Prog. Polym.Sci.,*37, 237 (2012).

[26]M. Ghoochian, H.A. Panahi, S. Sobhanardakani, L. Taghavi, A.H. Hassani, *Microchem. J.*,145, 1231(2019).

[27]M. Ghoochian, S. Sobhanardakani, H.A. Panahi, L. Taghavi, A. Hassani, *J.Water Wastewater,*30, 49 (2019).

[28]Y. Fu, W.J. Kao, *Exp. Opin. Drug Deliv.,*7, 429 (2010).

[29]M. Pooresmaeil, H. Namazi, *Int. J. Biol. Macromol.,*162, 501 (2020).

[30]A.I. Rezk, F.O. Obiweluozor, G. Choukrani, C.H. Park, C.S. Kim, *Int. J. Biol. Macromol.,*141, 388 (2019).

[31]J.M. Unagolla, A.C. Jayasuriya, *Eur. J.Pharmaceutical Sci.*,114, 199 (2018).

[32]N. Zirak, A.B. Jahromi, E. Salahinejad, *Ceramics Int.,*46, 508 (2020).

[33]I.B. Pathan, C.M. Setty, *Acta Pharmaceutica Sci.,* 53, 127(2011).

[34]L.A.D. Silva, E.R. Cintra, E.C.P. Alonso, G.L. Alves, E.M. Lima, S.F. Taveira, M.S.S. da Cunha-Filho, R.N. Marreto,*J. Thermal Anal. Calorimetry,*130, 1593 (2017).

[35]H.S. Vaziri, A. Shokuhfar, S.S.S. Afghahi, *Mater. Res. Express,*7, 025034 (2020).

[36]F. Yan, Z. Sun, J. Xu, H. Li, Y. Zhang, *Microchimica Acta,*187, 344 (2020).

[37]Y. Qin, Y. Peng, W. Yang, Y. Wang, J. Cui, Y. Zhang, *IOP Conf. Ser.: Mater. Sci. Eng.,* 770, 012079 (2019).

[38]Y. Guo, S. Guo, J. Ren, Y. Zhai, S. Dong, E. Wang, *ACS Nano,*4, 4001 (2010).

[39]J. Wang, Z. Guo, J. Xiong, D. Wu, S. Li, Y. Tao, Y. Qin, Y. Kong, *Inter.J. Biolog. Macromolec.,*125, 941 (2019).

[40]Y. Liu, Z. Lai, P. Yang, Y. Xu, W. Zhang, B. Liu, M. Lu, H. Chang, T. Ding, H. Xu, *RSC Adv.*7, 43104 (2017).

[41]H.R. Verma, K.K. Singh, T.R. Mankhand, *Waste Management,*60, 652 (2017).

[42]P. Yan, A. Liu, Y. Chen, J. Wang, S. Ruan, H. Chen, J. Ding, *Scientific Reports,*5, 12587 (2015).

[43]K.P. Sambasevam, S. Mohamad, N.M. Sarih, N.A. Ismail, *Inter.J.Molec.Sci.*14, 3671 (2013).

[44]I. Shown, S. Banerjee, A. Ramchandran, K.E. Geckeler, C. Murthy, *Macromolec.Symposia,*287, 51 (2010).

[45]K. Bauri, S.G. Roy, S. Arora, R.K. Dey, A. Goswami, G. Madras, P. De, *J.Thermal Anal.Calorimetry,*111, 753 (2013).

[46]H. Wei, X. Zhang, C. Cheng, S.X. Cheng, R.X. Zhuo, *Biomater.,*28, 99 (2007).

[47]H.H. Shin, H.W. Choi, J.H. Lim, J.W. Kim, B.G. Chung, *Nanoscale Res. Lett.,*15, 1 (2020).

[48]A.M. Alkafajy, and T.M. Albayati, *Mater. Today Commun.,*23, 100890 (2020).

[49]M.L. Bruschi, Strategies to Modify the Drug Release from Pharmaceutical Systems, Woodhead Publishing (2015).

[50]C. Jacques, H. Hopfenberg, V. Stannett, *Polym. Sci. Technol.,* 6, 73(1974).

[51]N.L. Thomas, A. Windle, *Polym.,*23, 529 (1982).